THE BALTIC JOURNAL
OF ROAD AND BRIDGE ENGINEERING

ISSN 1822-427X / eISSN 1822-4288
2017 Volume 12(1): 21–29

COMPREHENSIVE STUDY ON UNDERSLUNG GIRDER BRIDGE UNDER DIFFERENT LOADING CONDITIONS

Ieva Misiūnaitė[1]✉, Algirdas Juozapaitis[2], Alfredas Laurinavičius[3]

[1]*Research Institute of Building Structures, Vilnius Gediminas Technical University, Saulėtekio al. 11, LT–10223 Vilnius, Lithuania*
[2]*Dept of Bridges and Special Structures, Vilnius Gediminas Technical University, Saulėtekio al. 11, LT–10223 Vilnius, Lithuania*
[3]*Dept of Roads, Vilnius Gediminas Technical University, Saulėtekio al. 11, LT–10223 Vilnius, Lithuania*
E-mails: [1] *ieva.misiunaite@vgtu.lt;* [2] *algirdas.juozapaitis@vgtu.lt;* [3] *alfredas.laurinavicius@vgtu.lt*

Abstract. The comprehensive study on the structural behaviour of underslung girder bridge is examined in this study through both numerical modelling and experimental 3D model tests. The structural design of steel bridges in many cases is governed by their ability to withstand asymmetric loading conditions. Three different symmetric and asymmetric load cases were investigated to capture the deformational and flexural response of the main girder. It was found that under distributed load the structural response of underslung girder bridge was similar to beam-column with intermediate elastic supports. The numerical model was validated against experimental data with good agreement perceived, allowing an extensive parametric study to be performed. The observed influence of initial geometric imperfections and nonlinearities are discussed. It was found that symmetric load governs the ultimate limit state. However, the asymmetric one takes over in the case of serviceability. Finally, the study presented herein summarises experimental investigations, numerical simulations and design proposals obtained through the recent few years research program, carried on to deepen the knowledge on the structural behaviour of underslung girder bridges.

Keywords: beam-column behaviour, elastic support, experimental investigation, geometric imperfections, moment amplification, structural response, underslung girder bridge.

1. Introduction

Underslung girder, like their counterparts, cable-stayed bridges couple functionality with aesthetics of architectural design that are often used as a symbol of exclusivity for the city or even for the region where they are situated. However, their attractive design requires special attention for multiple factors such as the increased bending moments at the intermediate supports and unfavourable deformations due to asymmetric loading or the influence of elastic supports on the overall stability of the bridge.

The beginning of the 19th century indicates the realisation that the distances spanned by simply supported beams can be increased using an eccentric external tension chord (Muttoni 2014). These observations induced the development of beam string structures (BSS) and solved many problems related to the roofing of big spaces like stadiums or sports halls (Xue, Liu 2009). Bridge designers quickly adopted BSS with increased number of the struts and proposed the novelty today known as underslung girder bridges (UGBs).

The first examples of underslung girder bridges refer to the mid of 20th century. Despite successful realisations (Castielertobel Viaduct, Switzerland; Neckar Viaduct, Germany; Baltschiederbrücke, Switzerland, etc.), which still serve the demands of their users, this unconventional type of bridge felt into oblivious. The reason tends to be a lack of knowledge of its structural behaviour, a scarcity of studies of structural forms and incredulity of public and reluctance of public authorities (Christodoulou, Lark 2007). The first attempts to embed underslung girder structures into the substructures of viaducts led to the conclusion that the structural arrangement of such type of bridges is more suitable for short to mid-spans with the average length of 50 m (Kasuga 2011). The span constraints became one of the reasons for underslung structural arrangements more often being used in the design of footbridges. By span length observation, the new era of underslung girder bridges started, and within the last fifteen years, more than twenty UGBs have been designed and constructed. From the other types of steel

doi:10.3846/bjrbe.2017.03

bridges, UGB distinguishes by the complex flexural and axial response of the rigid beam caused by external forces and direct anchorage of the supporting system.

There are not many investigations carried out on the structural behaviour of underslung structures. Saitoh and Okada (1999) presented the survey on the hybrid string structures. In their work researchers mainly dealt with the role of strings, the tensile force in them, stress and displacement control by prestressing and classification of hybrid string structures. The most relevant studies possible to find in the literature, more recently, consider either prestressed concrete beams or steel stayed columns. Chan *et al.* (2002) introduced his numerical investigation on prestressed stayed columns stability check. In their work, researchers accounted for the second-order effects as well as initial imperfections. The study provides some parametric highlights on the influence of initial imperfections, rigidity and length of strut and dimensions of the stays as the reference for the designers. Since stability tends to be one of the main issues in stayed structures design, Saito and Wadee (2008) presented their study on the post-buckling behaviour of steel stayed columns. They found that the post-buckling behaviour is strongly dependent on the level of the initial pre-stress. Consequently, experimental verifications followed the numerical attempts to predict the structural behaviour of the stayed structures. De Araujo *et al.* (2008) presented a study embedding ANSYS numerical calculations and a series of full-scale tests. Some of the main contributions of their study related to the conception, development, and execution of 3D experimental investigation and finite element (FE) models calibration by using experimental data, as well as, focus on the governing parameters that could affect the structural response. Recently Serra *et al.* (2015) performed a comprehensive study on 12 steel prestressed stayed columns. Researchers performed 44 experimental tests in order to obtain the data on the compressive strength and behaviour of such systems by varying cross-section geometry, the diameter of cables, initial pretension level of stays and steel grade. Earlier Saito and Wadee (2009) examined the buckling behaviour of steel stayed columns with geometrical imperfections, and stress limitation relating to possible material failure. Their studies tend to show that such structures are the most sensitive to imperfections at a prestressed level that yields the highest critical load. The observations of these scholars led to the assumption that underslung structures supported by the non-prestressed stays are less sensitive to geometrical imperfections. Wu (2008) looked at the underslung structures from the different angle and put his efforts on an investigation related to the effect of the struts as indirect supports to reduce the bending moments in the beam. Another work dedicated to indirect supports by using cable-stayed systems refers to Wu and Sasaki (2007) attempt to stiffen the arch. Their paper investigated both static and dynamic behaviour of a cable-stiffened arch using numerical and experimental methods. It showed the possibility significantly to increase damping ratio of an arch by adding the cables. Also reviled the dependence of the damping ratio of the amplitude of the displacement and pre-stress of the cables. According to the survey of authors of this paper, one of the first studies related to UGBs belong to Muttoni (2014) and resulted from his consultant activity as a structural engineer in Switzerland during conceptual design of some UGBs. The increasing number of successful underslung girder bridge projects and acknowledgment among the engineers and public authorities encourage the researchers to fill the gap in the studies related directly to this type of bridge. In the last decade, the research of stayed structures turned to comprehensive studies dedicated to the steel-concrete composite UGBs. Ruiz-Teran and Aparicio (2007a) introduced two new types of bridges, naming them as under-deck cable-stayed (UDCS) and combined cable-stayed bridges. The under-deck cable-stayed bridge directly refers to the underslung beam structure as the others combine the underslung girder with the conventional cable-stayed bridge. The scholars also described the parameters governing the structural response of reinforced concrete deck of under-deck cable-stayed bridges (Ruiz-Teran, Aparicio 2007b). Meng and Zhang (2014) also worked on the structural performance of a combined cable-stayed bridge (CCSB). They preliminary study showed the advantages of the innovative structure to be such as decreased bending response and deflection, smaller cable forces, better dynamic resistance and all that lead to less amount of material. Later, there were determined the design criteria for short and medium span composite underslung girder bridges with prestressed stays (Madrazo-Aguirre *et al.* 2015a). The same group of researchers studied the dynamic behaviour of steel-concrete underslung girder bridges (Madrazo-Aguirre *et al.* 2015b) and suggested the computational method for UDCSBs nonlinear buckling and post-buckling check based on energy principles (Madrazo-Aguirre *et al.* 2015c). Camara *et al.* (2014) presented work on verification of the serviceability limit state of vibrations due to traffic loads in UGB. Throughout the parametric study employing an innovative vehicle-bridge interaction model, the authors showed that slender UGBs are highly sensitive to traffic loads induced vibrations.

This study aims at providing a broader grasp on the flexural and deformational behaviour of UGB and its design. It presents the numerical results obtained through nonlinear analysis using initially imperfect and additionally elastically supported beam-column mathematical model and two amplification factor techniques covering the second order effects for the first order calculations. The load cases adopted by the study cover maximum nominal symmetric load and two asymmetric loads based on analytic and engineering approach, respectively. In particular, research draws some interesting conclusions on the application of design amplification methodologies.

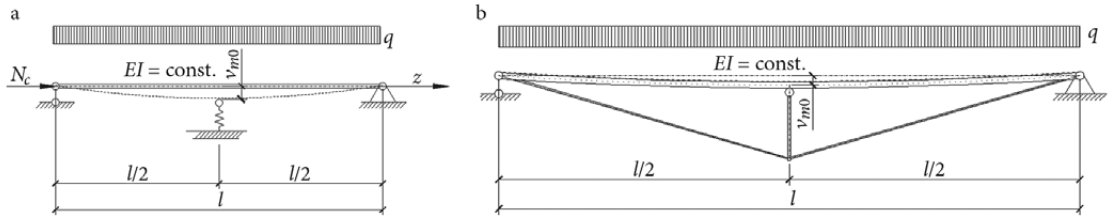

Fig. 1. Underslung girder bridge: a – mathematical model; b – calculation model

2. Finite element modelling and basic assumptions

The FE software ANSYS was used for the numerical investigation. The numerical FE model, presented in Fig. 1b, reflects the mathematical model of simply supported initially imperfect beam-column with the intermediate elastic support presented in Fig. 1a. The mathematical model used for the FE simulations was based on the following assumptions:

– the elastic material model shall be used for all elements of the structure;

– the internal forces and moments shall be determined to take into account the deformed geometry of the structure;

– the assumed shape of local imperfections shall reflect the elastic buckling mode, which is given by

$$v_0 = v_{m0} \sin\left(\frac{\pi z}{l}\right), \tag{1}$$

where v_{m0} – the amplitude of the equivalent initial imperfection;

– the amplitude of the equivalent initial local bow imperfections and residual stresses by introducing generalised imperfection factor has the form of

$$v_{m0} = \frac{\alpha\left(\overline{\lambda} - 0.2\right)}{\overline{\lambda}^2}\frac{W}{A}, \tag{2}$$

where α – an imperfection factor which shifts the buckling curve for different cross-section types, sizes, thicknesses, buckling axes, and material strengths, given in *Eurocode 3: Design of Steel Structures – Part 1–1: General Rules and Rules for Buildings*; $\overline{\lambda}$ – non-dimensional slenderness, which is based on the relevant buckling curve; W and A – section modulus and cross-section area, respectively;

– the structure shall be assembled of slender members with the $\overline{\lambda} > 1$ in order to fail by elastic buckling.

The assumptions used for the mathematical model coincide with the requirements for the Geometrically Nonlinear Analysis with Imperfections (GNIA), which was used for the FE simulations. Fallowing previously described mathematical model the closed shape of the triangle was used to model the underslung girder bridge. Due to the direct anchoring of the stays, under applied distributed load the underslung beam was subjected to simultaneous bending and compression. The strut at the mid-span of the underslung beam prevents its structural deformations reflecting the elastic support used in the mathematical model. The second order effects were taken into account by performing a large deformation analysis. To simulate the initial imperfections, the spline type curved elements, having a sine script, were used, with the amplitude resulting from the Eq (2). Two types of beam (2D and 3D) elements models and one detailed solid elements model were used for the numerical simulations to identify the influence of the modelling accuracy to the exactitude of the results. The analysis led to minor differences among the calculation models, thus to avoid unnecessary modelling difficulties, the simplest 2D computational model was chosen for the numerical calculations.

3. Test setup and testing method

An experimental program was designed and implemented to evaluate the performance of the underslung girder bridge under different loading stages and conditions in the *Structural Engineering Lab at Vilnius Gediminas Technical University*. A three-dimensional underslung girder bridge model was designed and fabricated based on the triangular structural arrangement and the limiting slenderness parameter for the rigid beams to capture the influence of the nonlinearities. Three separate tests, identified as A, B and C were conducted on the experimental model of the bridge to examine its structural behaviour during service and ultimate loading conditions.

For underslung girder bridge structures, bending moments, when interacting with axial force, always govern the structural behaviour of the structure. Usually, the axial response does not exceed 20% of the total stress found in the underslung girder. Thus, this study focus on the flexural and deformational response of the structure. To capture bending moment distribution through the length of the girder totally 16 longitudinal strain gauges were installed on the both sides of the girder at sections S1 to S8. For the broader grasp of the structural behaviour of the bridge, additionally, one by one strain gauges were attached to the bottom of the stays and side of the strut. Fig. 2a shows the full set up of the strain gauges on one of the underslung girders. The displacement sensors were installed on the bottom of the girder at sections I1-I8 and the end of the strut as shown in Fig. 2b to evaluate the deformational behaviour of the underslung girder bridge.

3.1. Experimental model design and fabrication

The underslung girder bridge experimental model was designed following the governing parameters and structural arrangement, which were used for the GNIA calculations as shown in Fig. 1. The simply supported bridge has a width of 0.8 m, a span of 4.0 m, and constitutes of two parallel plane underslung girder structures. The bridge has a bracing block at the mid-span to prevent lateral deformations and to maintain plain structural behaviour. The beams, struts and the braces were made of the cold formed hollow sections, and the stays were formed using a hot rolled steel strip. Table 1 lists the geometric properties of all bridge model elements.

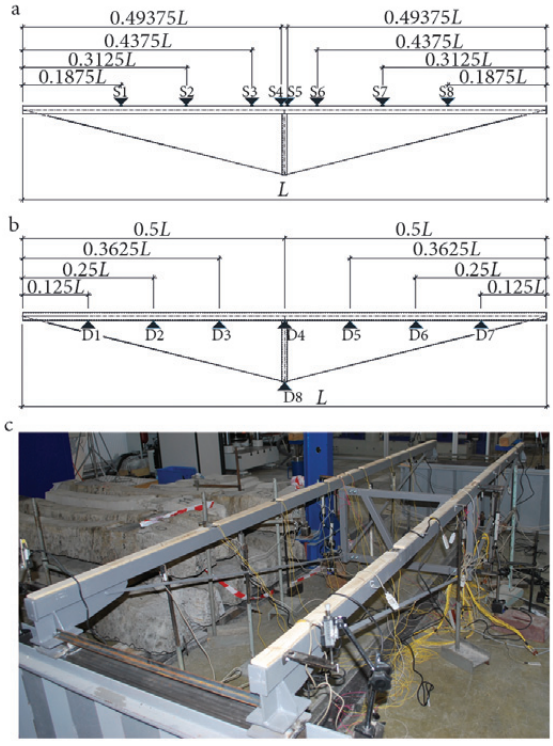

Fig. 2. Test set up: a – arrangement of the strain gauges; b – displacement sensors; c – experimental model in the Lab

Table 1. Parameters of the experimental model

Parameter		Value
Overall dimensions	Total length, mm	4000
	Left side, mm	2000
	Right side, mm	2000
	Length of the strut, mm	500
	Width, mm	800
Rigid beams	Cross-section area RHS 60×40×2, mm^2	374
	Moment of inertia, mm^4	184 100
	Modulus of elasticity, N/mm^2	210 000
Struts	Cross-section area SHS 40×40×2, mm^2	294
	Modulus of elasticity, N/mm^2	210 000
Stay cables	Cross-section area Strip 25×4, mm^2	100
	Modulus of elasticity, N/mm^2	210 000

All the connections of the fabricated structures were made throughout the welded gusset plates. The nominal yield strength of all elements and plates was 355 N/mm^2. The 3D experimental bridge model, presented in Fig. 2c was assembled in the laboratory, using the bracing block to connect two plain underslung bridge structures.

Initial global geometric imperfections of the both rigid beams of the bridge were measured before each of the tests. A simple thin wire was used to obtain the magnitude of the initial imperfection at mid-length of the underslung girder's elements. The geometric imperfections were taken as the deflection of the top surface of the cross-section. The sign convention and the location of the measurement correspond to the ones shown in Fig. 1. The measured values of the global geometric imperfections at the mid-length of the rigid beams were 4.1 mm and 5.6 mm before Test A, 4.6 mm and 5.7 mm before Test B and 3.7 mm and 5.1 mm before Test C, respectively. These measured values in most of the cases were slightly smaller when compared to calculated value of the initial local bow imperfection by using Eq (2) which was 5.66 mm.

3.2. Test A – symmetric loading

The experimental model was tested under incremental symmetric load, which induced bending moments reflecting those, which represent the design code based bending capacity, to evaluate the structural behaviour of the underslung girder bridge under ultimate load. To avoid the possible breakage of the displacement transducers under deformation of the structure, they have been removed before applying the ultimate load at the load step 10. Experimental rearrangement resulted in the maximum displacement obtained at the load equal to 3.44 kN/m, which amounts to 81% of the maximum applied load (Misiunaite, Juozapaitis 2014). The loads for all cases considered have been implemented by hand using the weights of approximately 10 or 20 kilos, following initially established scenario and going from opposite ends to mid-section simultaneously. For the distribution of the weights, there were used wooden pallets, which weight refers to the first load step. Fig. 3 summarises the loading history of the symmetric distribution of the weights. The uneven weight of the loading weights resulted in varying values of the loading increments as well as the speed of loading. Each load step was followed by approximately 20 s of data recording, which appears as horizontal lines in a chart of loading history. After the 10th load step, which equals to a load of 3.44 N/mm, loading was performed in the smaller increments, to avoid the sudden breakage of the structure. The ultimate load was extended in 16 load steps. After the nominal yield stress was reached, still no failure occurred, and the structure was reloaded. At the end of the test no evident plastic deformation were observed in the structure.

3.3. Test B – Analytic asymmetric load approach

The experimental model was tested under incremental asymmetric load, by keeping the asymmetry at each load step to

compare the behaviour of the underslung girder bridge with the previously obtained numerical data. A horizontal incremental load was applied on the top of a wooden deck to obtain transversally distributed load on the underslung girders. Applying a horizontal load to the top of the wooden deck induced a moment and axial compression in the underslung girders. The laterally distributed load was simulated by orderly placing weights of 20 kg and 10 kg. Both loading and reloading of the bridge were performed in five steps. Only first load step refers to the symmetric load by means of the weight of wooden pallets. Fig. 4 details the loading history of Test B and embeds two charts; each of them represents the loading process on the mid-span of the bridge. The less load value represents the dead load, and the higher one is the sum of dead and live loads. The loads applied were recorded by counting the weights. The maximum dead load applied on each underslung girder was 1.37 kN/m, and the total sum of dead and live loads tend to be 2.6 kN/m, thus giving dead to live load ratio equal to 1.11.

3.4. Test C – Engineering asymmetric load approach

The experimental model was tested under a combination of symmetric dead and asymmetric live load to evaluate the structural behaviour of the underslung girder bridge using asymmetric engineering load. The engineering load approach covers the real bridge loads appearing during its execution and use. Fig. 5 depicts the loading history of Test C and employs two charts, each of them representing the load applied on one of mid-span of the bridge. The total dead load was applied in two steps and had a maximum value of 1.5 kN/m. It was laterally distributed on each of underslung girders using the wooden deck. The total live load was applied in two sequential steps and had a maximum value of 2.13 kN/m. It was distributed on one-half of each of underslung girders. The dead to live load ratio used for Test C was 2.38.

4. Experimental and numerical results

The flexural and deformational response of an underslung girder bridge is a useful measure of the parameters reflecting the structural behaviour of the underslung girder. Fig. 6 summarises numerical and experimental results of the flexural response of UGB under symmetric load conditions. The plots provide the variation of the in-plane bending moment (M) with the length (L) of the underslung beam. Fig. 6 also depicts the results of the comparison analysis embedding ANSYS nonlinear vs linear static calculations, together with the experimental results and two alternative design techniques covering assessment of the bending moments in *Eurocode 3* interaction formulae. The area plot shows the in-plane bending moment

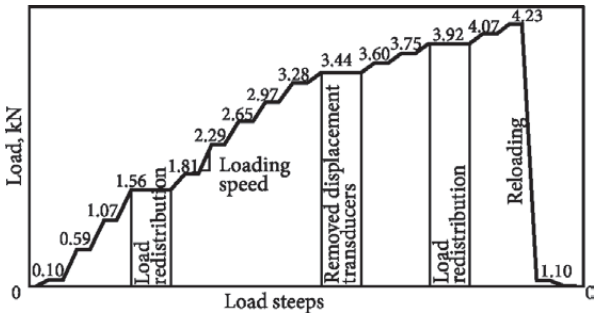

Fig. 3. Loading history of the symmetric load

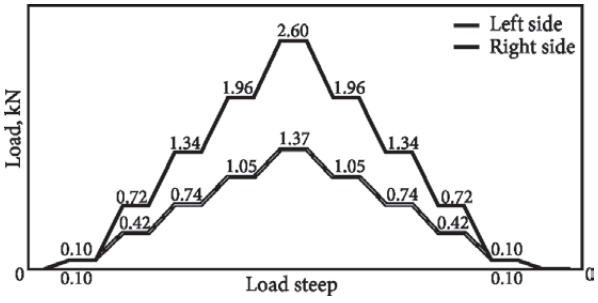

Fig. 4. Loading history of the analytical asymmetric load

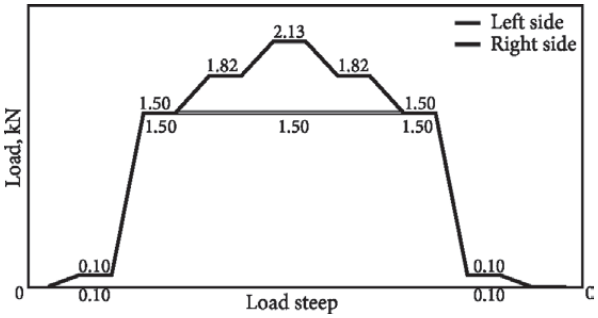

Fig. 5. Loading history of the engineering asymmetric load

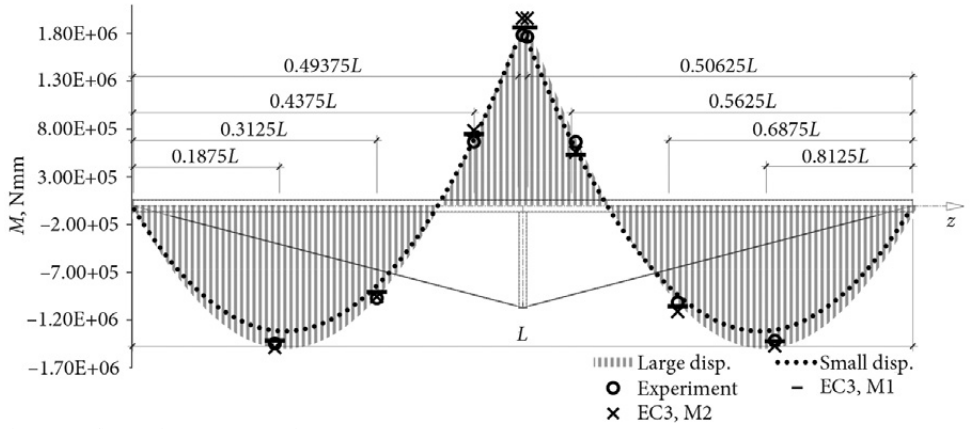

Fig. 6. Results of the UGB flexural response under Test A

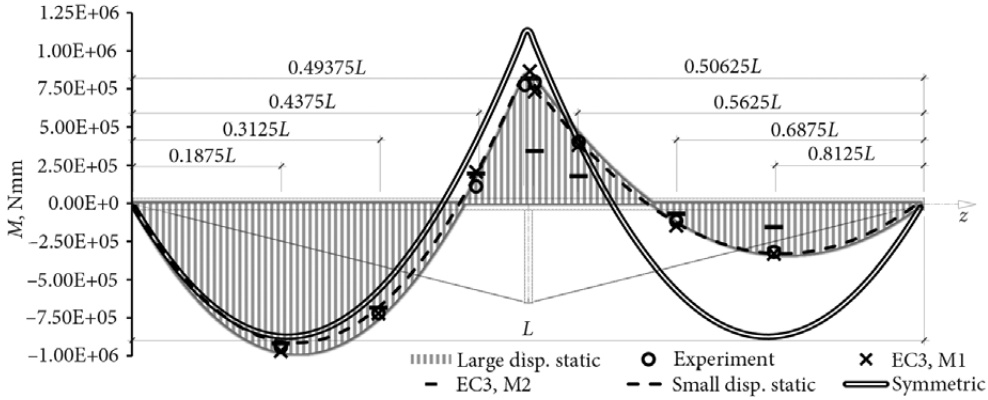

Fig. 7. Results of the UGB flexural response under Test B

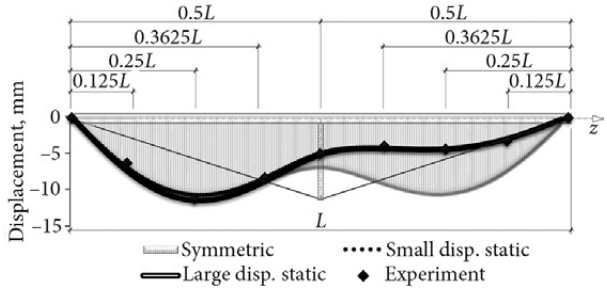

Fig. 8. Results of the UGB deformational response under Test B

variation obtained using GNIA based ANSYS large displacement static analysis. The dotted curve gives the results of ANSYS small displacement static analysis and different scatter marks represent the bending moment values obtained during the experimental investigation and using two alternative methods provided by *Eurocode 3*, known as Method 1 and Method 2. The experimental results with the sufficient accuracy validate the numerical GNIA calculations. The errors for the maximum sagging moments do not exceed 9% and for hogging ones – 3%. Fig. 6 represents the obvious difference between linear and nonlinear results, which is 11% for maximum sagging and 14% for maximum hogging moments, respectively. The track of the design specifications by using amplification factors to cover the second order effects decreases the errors of linear calculations to 2% and 5% for hogging and sagging moments of Method 1 and to 3% and 0% in the case of Method 2. Comparison of the bending moment values given by design specifications to experimental results yields to 4% and 2% errors of hogging and sagging moments in case of Method 1 and to 9% and 3% for the Method 2.

Next, Fig. 7 provides the flexural response results of Test B. The results presented concern underslung girder bridge under asymmetric load using GNIA calculations, small displacement static analysis, and moment amplification covered by both Method 1 and Method 2, as well as experimental verification, and bending moment distribution under a symmetric load of 2.6 kN/m. Asymmetric nonlinear calculations yield 13% more sagging moments in comparison to symmetric ones. However, the hogging moment at mid-section is 23% more due to symmetric load, and thus the symmetric load governs the design limit state of underslung girder bridge. Moreover, symmetric vs asymmetric load case comparison displays the obvious difference in sagging to hogging bending moment transition. Experimental validation of GNIA calculations yields 3% and 5% errors for maximum left and right side sagging moments, respectively, and 8% errors for hogging moments at the mid-span. Numerical calculations tend to be slightly more conservative and in good agreement with experimental results. Due to relatively small loading, the nonlinear vs linear analysis gives just 5% error of maximum left side sagging and minor 2% errors for hogging and maximum right hand sagging moments. Method 1 amplification factors shift the maximum left and right side sagging and hogging moments closer to the nonlinear calculations withdrawing only 1% error. The verification of Method 1 design methodology concludes to 3% and 4% left and right side maximum sagging moments, as well as 8% errors of hogging moments. All the values obtained by Method 1 tend to be slightly more conservative in comparison to experimental results. Fig. 7 depicts controversial results of the calculations using Method 2. For the left side of the considering structure, experiencing the bigger values of bending moments, comparison to nonlinear calculations give the accuracy of the results with 6% and 1% conservative errors for sagging and hogging moments, respectively. It is evident, that Method 2 is not sufficient for such kind of structures design under asymmetric load, as, for the right side of the structure; the amplification factors shift the first-order values of bending moments far away from experimental and analytical results. Method 1 based on second-order in-plane elastic theory more closely coincides with the mathematical model used for the underslung girder bridge analysis, and therefore better matches the data.

Figure 8 depicts the deformational response of the underslung girder bridge by grasping the values obtained from Test B asymmetric load together with the ones given by symmetric load of 2.6 kN/m. The area chart represents the vertical displacement variation within the length of the underslung girder. The double and dot lines refer to nonlinear and linear calculation results, respectively and the scatter provides the experimental verification. In

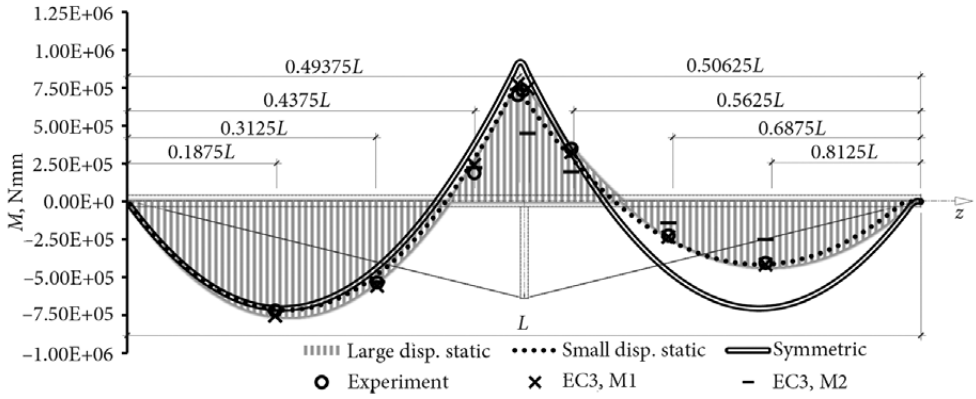

Fig. 9. Results of the UGB flexural response under Test C

contrast with the results of ultimate limit state, the deformations derived by the asymmetric load govern the serviceability limit state, as maximum displacement provided by symmetric load tends to be 8% less than asymmetric one. Nonlinear vs linear calculations outline minor errors decreasing from 7% to 2% by going from heavily to lightly loaded side of the structure. For the real design cases, when the structures are more slender and the dead to live load ratio is less the difference between linear and nonlinear calculations dramatically increases (Misiunaite *et al.* 2012). Moreover, inversely to the design check, there are no amplification factors to shift linear displacements closer to nonlinear one, thus for accurate and safe design GNIA becomes mandatory. Especially taking into account, that serviceability limit state usually governs the design process of short to mid-span UDGBs. The verification of GNIA calculations resulted in high accuracy with 2% and non-error for the maximum displacement of the left and right side, respectively. The GNIA displacement at the mid-span of the bridge turned to be 3% less than the experimental one.

Figure 9 details the flexural response of the underslung girder bridge under Test C and 2.13 kN/m symmetric load. Bending moment variation within the length of the girder resulted in the same tendency as for the previously described case of Test B. As expected; the experimental verification introduces marginally bigger errors comparing to analytic loading case. The values determined using large displacement static analysis of ANSYS turned to be conservative and varying from 5% to 9% for sagging and hogging moments of the heavily loaded side and 2% to 6% of the lightly loaded one. The greater difference of dead to live load ratio resulted in less difference between symmetric and asymmetric bending moments. Concerning Test B, the difference between symmetric and asymmetric values of maximum sagging and hogging moments decreased to 7%, and 16%, respectively. Despite that, the structure tends to behave in the same way, asymmetric sagging moments are bigger than symmetric, and vice versa with the hogging ones, thus still the symmetric values govern the structural design of the bridge. The nonlinear vs linear comparative analysis resulted in 8% to 10% difference

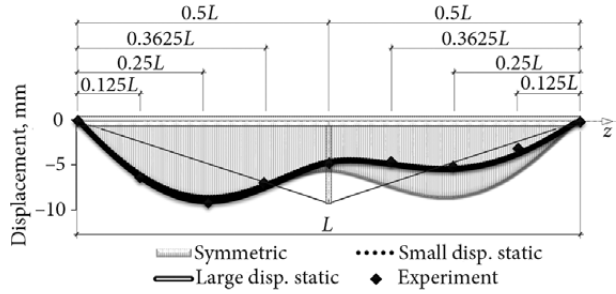

Fig. 10. Results of the UGB deformational response under Test C

between sagging and 4% difference between hogging moments. Method 1 amplification factors shift linear bending moments closer to nonlinear ones with a very high accuracy and neglected difference of 0% to 1% for sagging to hogging moments for more loaded side and 4% to 2% difference for sagging to hogging moments on the less loaded side of the bridge. Being very close to GNIA results the design values of Method 1 are also in good agreement with the experimental data. Method 2 follows the same scenario, already presented in Fig. 7. For the heavily loaded side of the structure, which as well experiences less differing maximum sagging and hogging moments, the amplifications shift the linear results closer to the nonlinear ones, and cause the errors of 5% and 4% in sagging and hogging parts, respectively. For a side of the structure affected only by dead load the methodology provides inadequate results.

Figure 10 shows the results of the deformational response under the Test C, as well as displacements distribution due to symmetric 2.13 kN/m load. The deformations observed during Test C tend to follow the scenario of Test B, presented in Fig. 8. The asymmetric displacements surpass the symmetric ones with 5% difference and govern the serviceability limit state. The experimental results validate the numerical calculations with just 1% difference for the left side maximum and mid-span displacement at 0.25*L* and 0.5*L*, respectively and provide a maximum 6% error for the right side 0.25*L* point displacement. Due to relatively high dead to live load ratio ($g/q = 2.38$) and small relative slenderness of the underslung girder ($\overline{\lambda} = 1.18$), the structure tends to be not very sensitive to nonlinearities,

and the comparison of large to small displacement static analysis resulted in moderately less 6% difference in maximum displacement.

5. Conclusions

The numerical and experimental program described in this study demonstrates the influence of the nonlinearities on the structural behaviour of underslung girder bridges, as well as the accuracy of the design techniques available in European codes commonly used to cover second-order effects and initial imperfections. The investigation has been carried out under maximum nominal symmetric load together with two asymmetric loads representing analytical and engineering point of view, respectively. The observation of all numerical and experimental results leads to the following conclusions.

1. For all symmetric and asymmetric load cases, structural behaviour of the rigid beam of underslung girder bridge shows clear sensitivity to nonlinearities.

2. Experimental investigation declares GNIA based numerical calculations to be safe and accurate for all considered load cases.

3. The comparison analysis of two amplification factors techniques, provided by *Eurocode 3* and known as Method 1 and Method 2, draw controversial results. For the case of symmetric load, both techniques turned to be accurate and reliable by shifting first-order values of bending moments close to nonlinear ones. On the other hand, for both asymmetric cases, Method 1, which is based on second order elastic theory worked perfectly. However, Method 2 embedding equivalent moment concept, turned to be inappropriate for underslung girder bridge design.

4. For all ultimate limit state checks, flexural response caused by symmetric load took over the asymmetric one. However, asymmetric vertical displacement governed the serviceability limit state. Thus, underslung girder bridges design requires careful consideration of both symmetric and asymmetric load cases.

References

De Araujo, R. R.; de Andrade, S. A. L.; da Silva Vellasco, P. C. G.; da Silva, J. G. S.; de Lima, L. R. O. 2008. Experimental and Numerical Assessment of Stayed Steel Columns, *Journal of Constructional Steel Research* 64(9): 1020–1029. https://doi.org/10.1016/j.jcsr.2008.01.011

Camara, A.; Nguyen, K.; Ruiz-Teran, A. M.; Stafford, P. J. 2014. Serviceability Limit State of Vibrations in Under-Deck Cable-Stayed Bridges Accounting for Vehicle-Structure Interaction, *Engineering Structures* 61(1): 61–72. https://doi.org/10.1016/j.engstruct.2013.12.030

Chan, S-L; Shu, G-P.; Lu, Z-T. 2002. Stability Analysis and Parametric Study of Pre-Stressed Stayed Columns, *Engineering Structures* 24(1): 115–124. https://doi.org/10.1016/S0141-0296(01)00026-8

Christodoulou, C.; Lark, R. J. 2007. Underslung Cable Structures – a Feasible Alternative? in *Proc. of the 5th International Conference on the Current and Future Trends in Bridge Design, Construction and Maintenance*. Ed. by Lark, R., 17–18 September, 2007, Beijing, China. CD-Rom, 351–359. https://doi.org/10.1680/bdcam.35935.0038

Kasuga, A. 2011. Development of a New Bridge Construction Method Using Suspension Structures, *Structural Concrete* 12(2): 65–75. https://doi.org/10.1002/suco.201000002

Madrazo-Aguirre, F.; Ruiz-Teran, A. M.; Wadee, M. A. 2015a. Design Criteria of Under-Deck Cable-Stayed Composite Bridges for Short and Medium Spans, *Structural Engineering International* 25(2): 125–133. https://doi.org/10.2749/101686615X14210663188574

Madrazo-Aguirre, F.; Ruiz-Teran, A. M.; Wadee, M. A. 2015b. Dynamic Behaviour of Steel-Concrete Composite Under-Deck Cable-Stayed Bridges under the Action of Moving Loads, *Engineering Structures* 103(15 November 2015): 260–274. https://doi.org/10.1016/j.engstruct.2015.09.014

Madrazo-Aguirre, F.; Wadee, M. A.; Ruiz-Teran, A. M. 2015c. Non-Linear Stability of Under-Deck Cable-Stayed Bridge Decks, *International Journal of Non-Linear Mechanics* 77(December 2015): 28–40. https://doi.org/10.1016/j.ijnonlinmec.2015.07.001

Meng, X.; Zhang, C. 2014. Extradosed and Intradosed Cable-Stayed Bridges with Continuous Cables: Conceptual Consideration, *Journal of Bridge Engineering* 19(1): 5–14. https://doi.org/10.1061/(ASCE)BE.1943-5592.0000477

Misiunaite, I.; Juozapaitis, A. 2014. Advances in Steel Under-Deck Cable-Stayed Bridges, *BTU Stahlbau-Symposium*, Cottbus, Germany, 2014, Heft 8: 25–32.

Misiunaite, I.; Daniunas, A.; Juozapaitis, A. 2012. Unconventional Double-Level Structural System for Under-Deck Cable-Stayed Bridges, *Journal of Civil Engineering and Management* 18(3): 436–443. https://doi.org/10.3846/13923730.2012.700106

Muttoni, A. 2014. Some Innovative Prestressed Concrete Structures in Switzerland, *Keynote lecture at the 23rd Symposium on Development in Prestressed Concrete.* Japan Prestressed Concrete Institute, Morioka, Japan, 2014, 12 p.

Ruiz-Teran, A. M.; Aparicio, A. C. 2007a. Two New Types of Bridges: Under-Deck Cable-Stayed Bridges and Combined Cable-Stayed Bridges. The State of the Art, *Canadian Journal of Civil Engineering* 34(8): 1003–1015. https://doi.org/10.1139/l07-017

Ruiz-Teran, A. M.; Aparicio, A. C. 2007b. Parameters Governing the Response of Under-Deck Cable-Stayed Bridges, *Canadian Journal of Civil Engineering* 34(8): 1016–1024. https://doi.org/10.1139/l07-016

Saito, D.; Wadee, M. A. 2009. Buckling Behaviour of Prestressed Steel Stayed Columns with Imperfections and Stress Limitation, *Engineering Structures* 31(1): 1–15. https://doi.org/10.1016/j.engstruct.2008.07.006

Saito, D.; Wadee, M. A. 2008. Post-Buckling Behaviour of Prestressed Steel Stayed Columns, *Engineering Structures* 30(5): 1224–1239. https://doi.org/10.1016/j.engstruct.2007.07.012

Saitoh, M.; Okada, A. 1999. The Role of String in Hybrid String Structures, *Engineering Structures* 21(8): 756–769. https://doi.org/10.1016/S0141-0296(98)00029-7

Serra, M.; Shahbazian, A.; da Silva, L. S.; Rabelo, C.; da Silva Vellasco, P. C. G. 2015. A Full Scale Experimental Study of Pre-

stressed Stayed Columns, *Engineering Structures* 100: 490–510. https://doi.org/10.1016/j.engstruct.2015.06.033

Wu, M. 2008. Analytical Method for the Lateral Buckling of the Struts in Beam String Structures, *Engineering Structures* 30(9): 2301–2310. https://doi.org/10.1016/j.engstruct.2008.01.008

Wu, M.; Sasaki, M. 2007. Structural Behaviors of an Arch Stiffened by Cables, *Engineering Structures* 29(4): 529–541. https://doi.org/10.1016/j.engstruct.2006.05.018

Xue, W.; Liu, Sh. 2009. Design Optimization and Experimental Study on Beam String Structures, *Journal of Constructional Steel Research* 65(1): 70–80. https://doi.org/10.1016/j.jcsr.2008.08.009

Received 25 July 2016; accepted 6 October 2016